EUSIPCO 2013 1569744517

CORRELATION AND VARIATIONAL APPROACHES FOR MOTION AND DIFFUSION ESTIMATION IN FLUORESCENCE IMAGING

Denis Fortun[1], *Chen Chen*[2], *Perrine Paul-Gilloteaux*[2], *François Waharte*[2], *Jean Salamero*[2], *Charles Kervrann*[1]

[1] Inria, Centre de Rennes - Bretagne Atlantique, 35 042 Rennes Cedex, France
[2] UMR 144 CNRS - PICT IBiSA - Institut Curie 75 248 Paris Cedex 05, France

ABSTRACT

In this paper we compare correlation-based and variational approaches for both motion and diffusion estimation in fluorescence imaging. The so-called Spatio-Temporal Image Correlation Spectroscopy (STICS) is widely used in fluorescence imaging to recover physical parameters such as directional flow or diffusion parameters of moving molecules. In addition, we have investigated recent advances in dense motion estimation techniques and their potential for applications in live cell fluorescence imaging. We propose a novel diffusion estimation method in a variational framework providing dense and discontinuity-preserving diffusion fields. The performances of the variational and STICS approaches are evaluated in three representative biological studies. In particular, we demonstrate the accuracy of STICS in stationarity conditions, and we point out the advantages of dense variational estimation to accurately recover spatial and temporal discontinuities. Pre-processing steps and parameters influence are emphasized in the variational framework.

Index Terms— optical flow, variational optimization, image correlation spectroscopy, fluorescence microscopy

1. INTRODUCTION

There is a growing interest for the use of live cell imaging for cancer research and analysis of the dynamical behavior of biological structures. A majority of approaches for motion analysis in biological sequences is based on individual tracking of biological objects [1]. However tracking methods are not adapted to answer to a set of biological questions, especially when the density and the lack of prominent features prevent the individual extraction of objects of interest undergoing complex motion (e.g. protrusions or membrane deformation in bio-mechanical studies). Accordingly, estimating the global deformation field can be more appropriate to capture complex dynamics observed in biological sequences [2, 3].

Some dense motion fields correspond to active transport of proteins but the main mode of transport is often diffusive, i.e. proteins undergo brownian motion. This type of motion is adequately modeled by its corresponding diffusion coefficient, representative of local change of the medium, or of the protein complex itself. In this paper we adress both the problems of estimating motion field and diffusion coefficient in time-lapse fluorescence microscopy.

In fluorescence imaging, the most popular techniques are based on correlation measures under the hypothesis of temporal stationarity of fluorescence signals [4, 5]. In this paper, we focus on the STICS method, representative of correlation-based methods for motion and diffusion estimation. We compare this correlation approach to variational principles [6] established as the state-of-the-art optical flow methods [7]. Global variational approaches have been recently investigated in biological imaging [3, 8].

Our contributions are (i) to adapt the well-established variational methods for optical flow to specific biological studies, emphasizing the need to adapt regularization parameter, data constraint and pre-processing step, (ii) to propose a variational model for the estimation of the diffusion coefficient, (iii) to provide qualitative and quantitative comparisons with the STICS technique usually recommended in fluorescence imaging. We demonstrate the potential of these two approaches in fluorescence imaging applications.

2. SPATIO-TEMPORAL IMAGE CORRELATION SPECTROSCOPY (STICS)

Image correlation spectroscopy approaches have been developed specifically for fluorescence microscopy, taking advantage of physical properties of fluorescent particles. These methods integrate the variations of fluorescence over space and/or time via correlation measures to access to information at the molecular level, such as diffusion coefficients or dominant flow speed and direction [4]. The generalized spatial and temporal correlation expression is defined as

$$r(\xi,\eta,\tau) = \frac{1}{N-\tau}\sum_{t=1}^{N-\tau} \frac{\langle \delta I(x,y,t)\ \delta I(x+\xi,y+\eta,t+\tau)\rangle}{\langle I(x,y,t)\rangle\langle I(x,y,t+\tau)\rangle} \quad (1)$$

where $I : \Omega \times [1,N] \to \mathbb{R}$ is an image sequence of N frames with Ω the image domain, $(\xi,\eta) \in \mathbb{R}^2$ are the spatial lags,

This work was realized as part of the Quaero Program, funded by OSEO, French State agency for innovation.

$\tau \in [1, N]$ is the temporal lag and $\langle\cdot\rangle$ is the spatial average over a patch. We define the intensity variation at pixel (x, y) at time t as $\delta I(x, y) = I(x, y, t) - \langle I(x, y, t)\rangle$. We point out that $r(\xi, \eta, \tau)$ is not a normalized correlation criterion but enables to recover the biophysical parameters associated to density, motion of molecules, and diffusion coefficient [4].

Motion estimation As with usual correlation-based techniques, the goal is to estimate the translation vector corresponding to the correlation peak maximum. In our experiments, the static or immobile molecule population is filtered by local averaging and $r(\xi, \eta, \tau)$ is computed by Fast Fourier Transform. We define

$$r(\xi, \eta, \tau) = r(\xi_p(\tau), \eta_p(\tau), \tau) e^{-\frac{(\xi-\xi_p(\tau))^2+(\eta-\eta_p(\tau))^2}{\omega_0^2}} + r_\infty(\tau), \quad (2)$$

where $r(\xi_p(\tau), \eta_p(\tau), \tau)$ is the t-lags maximum amplitude inversely proportional to the density in molecules, $r_\infty(\tau)$ is the spatial lag offset and ω_0 is the laser beam size which depends on the microscope. We denote $(\xi_p(\tau), \eta_p(\tau))$ the updated location of the correlation peak. Linear regression is then used to find the velocity vector from $(\xi_p(\tau), \eta_p(\tau))$. We consider a 2D Gaussian function to estimate accurately the correlation peak over time [4] using a Levendberg-Marquardt optimization scheme. In the experiments, the analysis is performed on image blocks. The size of the blocks determines the scale of moving objects retrieved and the maximum complexity of the estimated deformation (we take 64×64 pixels block size). The spatial lag between blocks is chosen to achieve an acceptable trade-off between spatial accuracy and computational time (we take 16 pixels spatial lag) (see Section 4).

Diffusion coefficient estimation In a diffusive motion scenario, the following diffusion equation is satisfied :

$$I_t = D_0 \, \Delta I \quad (3)$$

where I_t is the temporal derivative of I, D_0 is the isotropic diffusion coefficient and $\Delta\cdot$ denotes the laplacian operator. In order to estimate the scalar value D_0 , we first compute the diffusion decay τ_d using the following equation obtained by combination of (1) and (3) (see [9] for details) :

$$r(0, 0, \tau) = r(0, 0, 0)(1 + \tau/\tau_d)^{-1} + r_\infty(\tau) \quad (4)$$

and $D_0 = \overline{w_0}/4\tau_d$ where $\overline{w_0}$ is the temporal average of w_0.

This correlation-based technique will be compared to the global variational approach described in the next section.

3. VARIATIONAL APPROACH FOR MOTION AND DIFFUSION ESTIMATION

Motion estimation In [9], Horn and Schunk have proposed to determine the dense flow estimate as the minimizer of a global energy functional composed of two terms:

$$\widehat{w} = \arg\min_w E_{data}(I, w) + \lambda_w E_{reg}(w) \quad (5)$$

where $w : \Omega \to \mathbb{R}^2$ is the dense motion field, E_{data} is a data term penalizing deviations from a data conservation assumption over time, E_{reg} is a regularization term enforcing smoothness of the flow field and $\lambda_w > 0$ serves as regularization parameter to balance E_{data} and E_{reg} contributions. A high value of λ_w allows to retrieve only dominant motions of large structures by smoothing the flow field, while a small value of λ_w tolerates repeated close spatial variations corresponding to small objetcs. Variational approach of the optimization problem (5) is based on solving the Euler-Lagrange equations.

For our experiments we use the data term of [6] based on the assumption of conservation of intensity and spatial gradient of the image. The spatial gradient constraint is robust to additive illumination changes, which is necessary for several biological applications. We define

$$E_{data}(I, w) = \int_\Omega (1-\gamma)\phi(\theta_0|\nabla I^T w - I_t|^2) + \gamma\phi(\theta_x|\nabla I_x^T w - I_{xt}|^2) + \theta_y|\nabla I_y^T w - I_{yt}|^2))dx, \quad (6)$$

where $\phi(z^2) = \sqrt{z^2 + \epsilon}$ is the regularized L_1 norm with $\epsilon = 0.001$, $\nabla\cdot$ denotes the spatial gradient operator, the subscripts $\cdot_x$, $\cdot_y$ and $\cdot_t$ are respectively the derivatives along the x, y and t axis, and θ_0, θ_x, θ_y are normalization coefficients defined as $\theta_0 = (I_x + I_y + a)^{-1}$, $\theta_x = (I_{xx} + I_{xy} + a)^{-1}$ and $\theta_y = (I_{yx} + I_{yy} + a)^{-1}$ where $a = 0.1$ avoids division by 0.

The regularization term penalizes high gradients of the motion field $w = (u, v)$ with the convex and discontinuity-preserving $\phi(\cdot)$. We obtain the following energy term:

$$E_{reg}(w) = \int_\Omega \phi(\|\nabla u\|^2 + \|\nabla v\|^2)dx. \quad (7)$$

We follow the minimization method of [6] by successively solving the Euler-Lagrange equations associated to the problem (5) at each level of a coarse-to-fine decompostion. The non-linearity due to the penalization function $\phi(\cdot)$ is removed by fixed point iterations and the remaining linear system is solved with SOR ("Successive Over Relaxation").

Diffusion coefficient estimation We propose to estimate the diffusion parameter in the variational framework described above. Rather than estimating a constant diffusion coefficient over patches as performed with the STICS method, we consider a dense diffusion field $D : \Omega \to \mathbb{R}$. The estimation problem is then formulated as

$$\hat{D} = \arg\min_D \left\{E'_{data}(I, D) + \lambda_D E'_{reg}(D)\right\} \text{ s.t. } D(x) \geq 0. \quad (8)$$

The data fidelity is given by the diffusion equation (3). A data term penalizing ponctual deviations from this constraint is of

Table 1. Error of estimated translational motion of the Flux phases obtained with STICS and variational method for two values of λ_w (each cell of the table reports Angular Error / Endpoint Error).

	Flux 1	Flux 2
STICS	0.744 / 0.0125	0.733 / 0.0126
Variational, $\lambda_w = 5$	0.728 / 0.0124	0.782 / 0.0133
Vatiational, $\lambda_w = 11$	2.20 / 0.0372	1.67 / 0.0281

the form $E'_{data}(I, D) = \int_\Omega \phi((I_t - D\Delta I)^2)dx$. However, pointwise measurements are insufficient because of the random nature of the diffusion process. Therefore we design a neighborhood-wise data penalization by assuming a constant diffusion coefficient $D(x)$ over a neighborhood of a pixel x. This approach is similar to the CLG method for optical flow [10]. The data term is defined as

$$E'_{data}(I, D) = \int_\Omega \phi(\mathbf{D}^\top J_\rho \mathbf{D})dx \tag{9}$$

with $\mathbf{D} = \begin{pmatrix} D \\ 1 \end{pmatrix}$ and $J_\rho = K_\rho * \begin{pmatrix} \Delta I^2 & -I_t\,\Delta I \\ -I_t \Delta I & I_t^2 \end{pmatrix}$.

The regularization term imposes smoothness of D :

$$E'_{reg}(D) = \int_\Omega \phi(\|\nabla D\|^2)dx. \tag{10}$$

The constraint $D(x) \geq 0$ is achieved by adding a logarithmic barrier to the energy of (8). the minimization procedure is the same as for motion estimation. Up to our knowledge, it is the first time a diffusion field is estimated by variational minimization of a global regularized energy.

Contrary to the STICS method, this variational approach produces dense diffusion fields. Spatial variations of diffusion can thus be recovered more accurately, in particular at diffusion discontinuities usually occuring across membranes. Another difference is that the variational method exploits only two frames for the diffusion estimation whereas STICS uses extended sub-sequences. This choice sharpens the detection of temporal diffusion changes. However taking more frames into consideration can also improve the robustness of the estimation inside constant diffusion phases, therefore the estimations are averaged in practice over each phase.

4. EXPERIMENTS

In this section, we present three different biological problems which necessitate motion or diffusion estimation. We compare the variational and STICS approaches and demonstrate their potential.

Temporally varying diffusion We simulated an image time sequence shown in Fig.1-a and composed of three phases: pure directional flow (North-East translation, 0.28μm/s),

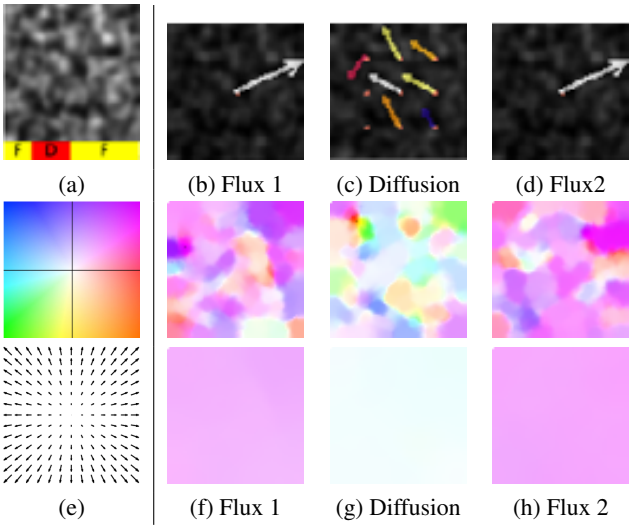

(a) (b) Flux 1 (c) Diffusion (d) Flux2

(e) (f) Flux 1 (g) Diffusion (h) Flux 2

Fig. 1. Analysis of STICS and variational method on synthetic image time series with three phases. (a) First frame of the sequence and temporal description of the 3 phases: F: Flux, D: Diffusion. (b,c,d) STICS analysis for each phase. The color legend is used to code the velocity value. (f,g,h) Variational estimation for image pairs of each phase with $\lambda_w = 5$ (first row) and $\lambda_w = 11$ (second row) (we set $\gamma = 0.75$). (e) Equivalence between the color-coded and vector visualization of motion fields.

Table 2. Detection of the three phases of the simulated sequence with STICS and variational method (each cell of the table reports begin frame / end frame of the phase).

	Flux1	Trans.	Diffusion	Trans.	Flux2
Ground truth	1/20	-	21/50	-	51/90
STICS	1/10	11/17	18/39	40/48	49/90
Variational	1/18	-	19/48	-	49/90

pure diffusion ($D = 0.01\mu\text{m}^2/\text{s}$), and pure directional flow (North-East translation, 0.28μm/s), respectively referred as Flux 1, Diffusion and Flux 2. This artificial example mimics a possible scenario observed in biological experiments with molecules in cells or beads in solutions. This simulation is used to demonstrate the ability of both methods to compute the dynamic parameters and to identify the three phases.

Figure 1 shows visual results obtained with STICS and variational methods. Two regularization parameters λ_w are compared in the variational case. We adopt two different motion visualizations : the motion vectors estimated every 16 pixels by STICS are represented by arrows, whereas the dense motion field of the variational method is more accurately visualized with the standard color-code presented in Fig. 1-e. The STICS exploits subsequences of 12 images.

The directional flow of Flux phases is well captured by the two methods. In the variational approach, small values for λ_w result in a detection of small moving structures. Higher values for λ_w allow us to recover the global flux, which is almost null

during the diffusion phase and constant (North-East direction) during the two Flux phases.

In Table 1, we have reported the Angular Error and End-point Error of motion estimations in the two flux phases (see [7] for definitions). The results show the high accuracy of STICS for estimating the Flux translation. With the variational approach, the translation is obtained by averaging the estimations at each pixel and for each frame of the Flux phases. We have reported the results in Table 1 for two regularization parameters. We notice that, in contradiction with the visual impression of Fig. 1, the estimated motion for $\lambda_w = 11$ corresponds to a high error, whereas for $\lambda_w = 5$, the error is consistent with the STICS method. This is due to the fact that large regularization coefficient favors smoothness against accuracy and tends to under-estimate the motion magnitude.

Based on this motion estimation, we identify the three phases. With the STICS method, we use backward and forward hidden Markov model on three states : Flux, Diffusion and Transition. With the variational method, a threshold is applied on the magnitude of the spatially averaged motion vectors of each frame to classify Flux and Diffusion phases. The classification results presented in Table 2 are consistent with the ground truth. Nevertheless, the STICS approach necessitates to consider a temporal analysis of a significant number of frames to produce satisfying diffusion estimation results. In our experiments, we processed 12 frames at each time point, which introduce a transition phase making the detection of transitions less accurate. The use of only two frames by the variational method allows to detect abrupt transitions.

Furthermore, the diffusion phase was analyzed separately to estimate the biophysical parameter related to diffusion rate. The diffusion coefficient of the diffusion phase was set to $D = 0.01\mu\text{m}^2/\text{s}$. The STICS estimates a coefficient $\hat{D} = 0.013\mu\text{m}^2/\text{s}$, and the variational methods estimates in average $\hat{D} = 0.016\mu\text{m}^2/\text{s}$. Thus, in this case of spatially constant diffusion, STICS achieves highest accuracy in the diffusion coefficient estimation.

Spatially varying diffusion To evaluate the ability of the variational approach to produce dense diffusion field and thus to accurately recover spatial diffusion changes, we simulated a spatially varying diffusion sequence. The particules density is the same in the whole image domain, as shown in Fig. 2-a, but the diffusion coefficient is higher inside the circle represented in Fig. 2-b ($D_1 = 0.1\mu\text{m}^2/\text{s}$) than outside ($D_2 = 0.01\mu\text{m}^2/\text{s}$). The parameters of the variational method are set to $\rho = 5$ and $\lambda_D = 500$.

The estimated diffusion field shown in Fig. 2-c is visually very close the ground truth. The two regions are clearly delimitated by the circle, despite an over-smoothing of the transition. The histogram of the diffusion field (Fig. 2-d) shows two modes corresponding to the two diffusion regions, but it also indicates that the diffusion inside the circle is under-

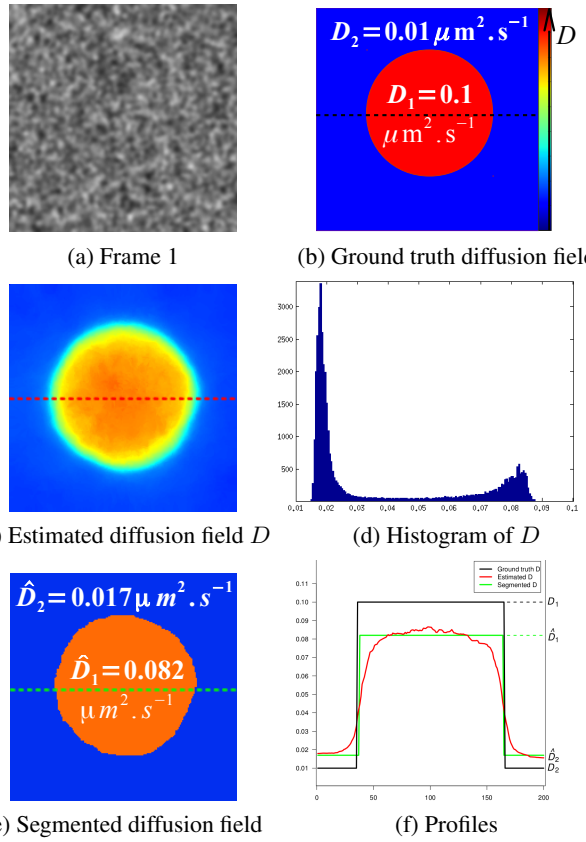

(a) Frame 1 (b) Ground truth diffusion field

(c) Estimated diffusion field D (d) Histogram of D

(e) Segmented diffusion field (f) Profiles

Fig. 2. Variational diffusion estimation on a simulated sequence with spatially variant diffusion. The curves of (f) are profiles of the dashed lines in (b),(c) and (e)

estimated. Figure 2-e shows the result of the mean-shift algorithm [11] applied to the diffusion field in order to delineate the two regions. Finally, 2D profiles of a line crossing the circle are represented in Fig. 2-d for ground truth, estimated and segmented diffusion fields. We observe that spatial discontinuities are accurately recovered, but $\hat{D}_1 = 0.082\mu\text{m}^2/\text{s}$ is slightly under-estimated, while $\hat{D}_2 = 0.017\mu\text{m}^2/\text{s}$ is slightly over-estimated.

The STICS method is enable to produce such dense diffusion segmentation map because of the spatial lag between the patches used to estimate diffusion. Besides, the large patch size leads to erroneous estimations near diffusion boundaries.

Cell deformation In the third experiment, we demonstrate the potential of the methods to quantify accurately cell deformation. Figure 3-a,b shows fluorescent protein GFP attached to a membrane protein Clathrin in spinning-disk confocal microscopy during chemical fixation. This sequence is also representative of other studies of deformations at the cell level. The interest of estimating motion in this case is to compensate the cell deformation involved in the chemical fixation process.

Analysis of velocities obtained by STICS shows that the main cell deformations are satisfyingly estimated. Due to the

time integration performed by the STICS method, we observe a regularization effect of the velocity map (Fig. 3-c,d). The dense map provided by the variational method successfully recovers detailed motions in the membrane and nucleus regions (Fig. 3-e,f). However, the motion estimated in these moving regions is propagated in static regions around the cell, whereas STICS is able to capture null motions. The variational estimation was affected by the abrupt change of fluorescence level between the two images (due to the pH change occurring during chemical fixation). We set the gradient constancy parameter $\gamma = 1$ in (6) to partially overcome this problem, but we still found beneficial to apply the image equalization method of [12] to improve the estimation. For a deformation compensation purpose, the accuracy of the motion estimation is of upmost importance, and is better achieved with the variational method.

5. CONCLUSION

In this paper we have evaluated a correlation-based approach and a variational method for motion estimation and diffusion estimation in live cell imaging. We have proposed a new variational diffusion estimation method able to recover spatially varying diffusion coefficients. STICS is block-based and takes advantages of a fitting model to recover the physical parameters. It is more robust to local fluorescence changes and more adapted for the estimation of spatially constant diffusion coefficient. The variational approach provides dense estimations of motion and diffusion fields. The motion and diffusion discontinuities are accurately recovered, and the adjustement of the regularization parameter allows to detect structures at several scales. Note that the size of blocks and the number of frames influence the estimation of motion and diffusion obtained by STICS as well. Combining these two approaches will be investigated in future works.

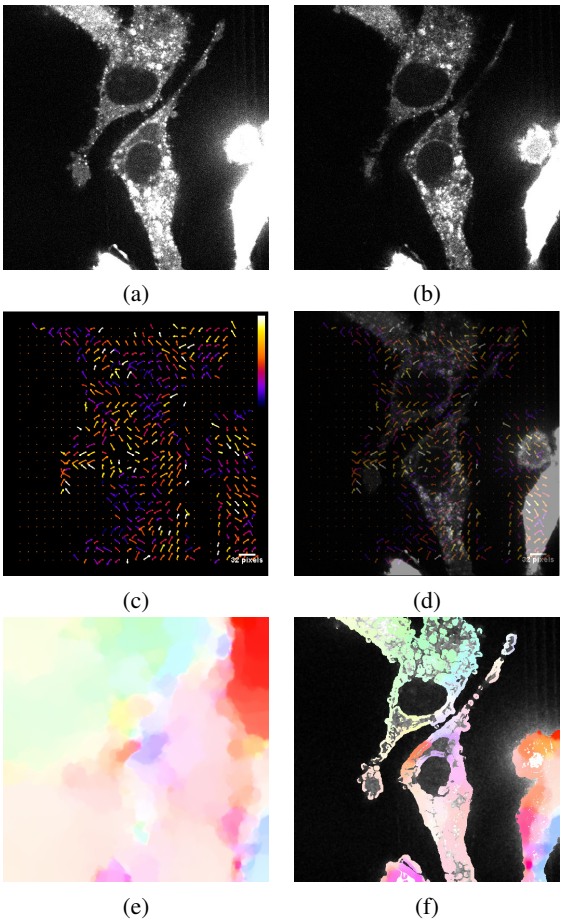

Fig. 3. Consequence of shrinking due to fixation of proteins Clathrin GFP. (a,b) Frames 0 and 100 of a temporal sequence of fluorescence images showing the cell membrane deformation. (c) Velocity map calculated by STICS over the whole sequence, and (d) the velocity map superimposed on the first frame. (e) Dense motion field obtained with the variational method ($\gamma = 1$, $\lambda_w = 11$), and (f) restriction of the visualization to regions of high spatial gradient amplitudes. Acquisition courtesy of PICT IBiSA UMR 144.

6. REFERENCES

[1] E. Meijering, I. Smal, and G. Danuser, "Tracking in molecular bioimaging," *IEEE Signal Proces. Mag.*, vol. 23, no. 3, pp. 46–53, 2006.

[2] I.-H. Kim, Y.-C.M. Chen, D.L. Spector, R. Eils, and K. Rohr, "Nonrigid registration of 2d and 3d dynamic cell nuclei images for improved classification of subcellular particle motion," *IEEE Trans. Image Processing*, vol. 20, no. 4, pp. 1011–1022, 2011.

[3] J. Delpiano, J. Jara, J. Scheer, O.A. Ramírez, J. Ruiz-del Solar, and S. Härtel, "Performance of optical flow techniques for motion analysis of fluorescent point signals in confocal microscopy," *Machine Vision Applications*, vol. 23, no. 4, pp. 675–689, 2011.

[4] B. Hebert, S. Costantino, and P.W. Wiseman, "Spatiotemporal image correlation spectroscopy (stics) theory, verification, and application to protein velocity mapping in living cho cells," *Biophysical J.*, vol. 88, no. 5, pp. 3601–3614, 2005.

[5] L. Ji and G. Danuser, "Tracking quasi-stationary flow of weak fluorescent signals by adaptive multi-frame correlation," *J. Microscopy*, vol. 220, no. 3, pp. 150–167, 2005.

[6] H. Zimmer, A. Bruhn, and J. Weickert, "Optic flow in harmony," *Int. J. Computer Vision*, vol. 93, no. 3, pp. 368–388, 2011.

[7] Simon Baker, Daniel Scharstein, J. P. Lewis, Stefan Roth, Michael J. Black, and Richard Szeliski, "A database and evaluation methodology for optical flow.," *Int. J. Comp. Vision*, pp. 1–31, 2011.

[8] Pizarro L., Delpiano J., Aljabar P., Ruiz del Solar J., and Rueckert D., "Towards dense motion estimation in light and electron microscopy," in *IEEE Int. Symp. Bio. Im.*, 2011, pp. 1939–1942.

[9] D.L. Kolin and P.W. Wiseman, "Advances in image correlation spectroscopy: measuring number densities, aggregation states, and dynamics of fluorescently labeled macromolecules in cells," *Cell Biochemistry and Biophysics*, vol. 49, no. 3, pp. 141–164, 2007.

[10] Andrés Bruhn, Joachim Weickert, and Christoph Schnörr, "Lucas/kanade meets horn/schunck: Combining local and global optic flow methods," *Int J. of Comp. Vis.*, vol. 61, no. 3, pp. 211–231, 2005.

[11] D. Comaniciu and P. Meer, "Mean shift: A robust approach toward feature space analysis," *IEEE Trans. Patt. Anal. Mach. Intel.*, vol. 24, no. 5, pp. 603–619, 2002.

[12] J. Delon, "Midway image equalization," *J. Math. Imaging Vision*, vol. 21, no. 2, pp. 119–134, 2004.